

Epitaxial growth of Zn₂Y ferrite films by pulsed laser deposition*

H. Kim^{a)}

School of Engineering and Applied Science, George Washington University, Washington, DC 20052

J. S. Horwitz, A. Piqué, H. S. Newman, P. Lubitz, M. M. Miller, D. L. Knies,
and D. B. Chrisey

Naval Research Laboratory, Washington, DC 20375

(Received 10 March 1999; accepted 18 June 1999)

Oriented and single phase Ba₂Zn₂Fe₁₂O₂₂ (Zn₂Y) thin films (~5000 Å thick) have been grown using pulsed laser deposition (ArF, 193 nm) on single-crystal (0001) sapphire substrates. A single phase polycrystalline Zn₂Y target was used to deposit films. The composition, structure, and morphology of the films were determined using Rutherford backscattering spectrometry, x-ray diffraction (XRD), and scanning electron microscopy. As a function of substrate temperature (>700 °C), films deposited in 200 mTorr of oxygen pressure were found to be deficient in Zn. The Zn deficiency increased with increasing substrate deposition temperature (<900 °C). Analysis of the XRD patterns indicated that films deposited from stoichiometric targets were primarily BaFe₁₂O₁₉ (BaM). Compensation of the target with excess Zn changed the structure of the film from BaM to a mixture of phases, i.e., BaM and Zn₂Y. Highly oriented and single phase Zn₂Y films could be achieved by depositing Zn₂Y film onto ZnO (~400 Å) buffered sapphire substrates. Deposited films exhibit an epitaxial relationship of (001)Zn₂Y//(001)ZnO//(001)Al₂O₃. The ferromagnetic resonance derivative linewidth of the Zn₂Y film for an in-plane applied field was ~310 Oe, which is larger than expected for bulk single crystals. © 1999 American Vacuum Society.

[S0734-2101(99)10405-6]

Ferrite frequency selective limiters are passive devices that protect microwave receivers from input damage by using the nonlinear excitation of magnetic spin waves.¹ In this type of limiter, signals that are above a critical rf magnetic field strength excite half-frequency spin waves in the ferrite, resulting in strong absorption of the rf power which is coupled to the crystal lattice and dissipated as heat. Currently, the technology is implemented exclusively in low loss, single-crystal yttrium-iron-garnet (YIG). The principal figure of merit for the ferrite limiters is the threshold power at which nonlinear absorption begins to take place. This critical rf field h_c in the parallel-pumped case, where the rf magnetic field is in the same direction as the dc magnetization, is given by

$$h_c \propto \frac{\Delta H_k \omega}{\gamma(4\pi M_s + H_a)}, \tag{1}$$

where ω is the signal radian frequency, ΔH_k is the spin-wave linewidth, $4\pi M_s$ is the saturation magnetization, $\gamma/2\pi = 2.8$ MHz/G, and H_a is the anisotropy field ($H_a \cong 0$ for YIG).^{2,3} A decrease in the threshold for limiting at a particular frequency can be achieved through either a reduction in the spin-wave linewidth or an increase in the saturation magnetization or a combination of both. Single-crystal YIG has

been reported as having an extremely narrow spin-wave linewidth, as low as approximately 0.25 Oe,¹ with $4\pi M_s \sim 1780$ G. An approach, which has the potential to dramatically reduce the ferrite limiter threshold, would be to substitute a hexagonal ferrite for YIG. Unlike YIG, hexagonal ferrites have large anisotropic magnetic properties. Magnetization values for the hexagonal ferrites Ba₂Zn₂Fe₁₂O₂₂ (Zn₂Y) are on the order of $4\pi M_s = 2850$ G and $H_a = 9900$ Oe.^{3,4} Assuming that an equally narrow spin-wave linewidth could be achieved in these materials (~0.25 Oe), according to Eq. (1), a reduction in the critical field by a factor of 7 is realized relative to YIG which would correspond to a factor of 50 reduction in the threshold power.

Zn₂Y is a hexagonal ferrite, different from BaFe₁₂O₁₉ (BAM) in that it has an easy plane of magnetization perpendicular to the c axis. Although there have been several reports⁵⁻⁸ on the properties of single-crystal bulk Zn₂Y hexagonal ferrites, there are not reports on the growth of Zn₂Y thin films. In this article, we report on the structure of the Zn₂Y thin films (grown by pulsed laser deposition (PLD) from single phase Zn₂Y targets) deposited on single-crystal (0001) sapphire substrates.

Films were deposited using an ArF excimer laser (Lambda Physics LPZ 305, 193 nm, 300 mJ per pulse). The laser was operated at 10 Hz and focused through a 50 cm focal length lens onto a rotating target at a 45° angle of

*No proof corrections received from author prior to publication.

^{a)}Corresponding author; electronic mail: hskim@ccf.nrl.navy.mil

TABLE I. Compositions of Zn₂Y films grown from various target compositions at different growth temperatures using RBS. Oxygen pressure was kept at 200 mTorr during deposition. High energy He ions at 6.45 MeV were used to separate the Zn and Fe signals for the Zn₂Y films. Film composition and thickness were determined using the RUMP simulation program (see Ref. 14).

Growth temperature (°C)	Target composition	Film composition
700	Ba ₂ Zn ₂ Fe ₁₂ O ₂₂	Ba _{1.6} Zn _{0.7} Fe ₁₂ O ₂₀
800	Ba ₂ Zn ₂ Fe ₁₂ O ₂₂	Ba _{1.6} Zn _{0.6} Fe ₁₂ O ₂₀
900	Ba ₂ Zn ₂ Fe ₁₂ O ₂₂	Ba _{1.6} Zn _{0.5} Fe ₁₂ O ₂₀
900	Ba ₃ Zn ₄ Fe ₁₂ O ₂₅	Ba _{1.5} Zn _{1.4} Fe ₁₂ O ₂₂
900	Ba ₄ Zn ₆ Fe ₁₂ O ₂₈	Ba _{2.9} Zn _{2.8} Fe ₁₂ O ₂₅

incidence. The focal spot size on the target was ~ 0.1 cm² which resulted in a fluence of ~ 1 J/cm² on the target. The target-substrate distance was 4.7 cm. The deposition rate of the films was 2–3 Å/s. The substrate was attached with silver paste to a stainless steel block, which was heated by two quartz lamps. The substrate temperature was monitored with a thermocouple at all times. The laser beam was rastered across the surface of the target with a computer-controlled mirror while the target was rotated.

Single phase Zn₂Y targets were prepared from ZnO, BaCO₃, and Fe₂O₃. The powders were mixed in a mechanical shaker for 30 min, pressed into a 2-cm-diam pellet at 7000 kg, calcined twice at 400 and 600 °C, crushed and pressed again, and then sintered at 1250 °C for 6 h. The substrates were cleaned in an ultrasonic cleaner for 10 min with acetone and then with methanol. All substrates were blown dry with dry nitrogen gas before they were introduced into the deposition system. After evacuating the chamber to a pressure of 10×10^{-5} Torr, the substrates were heated to the desired temperature in the desired oxygen pressure. During the deposition, oxygen background gas was introduced into the chamber to maintain a pressure of 50–400 mTorr. After deposition, the films were cooled to room temperature in 1 atm of oxygen. Some of the Zn₂Y films were postdeposition annealed at 900 °C for 2 h in flowing oxygen. Pairs of films were placed face to face during the anneal. The film thickness was measured by masking a portion of the substrate during deposition and then using a profilometer to measure step height. The deposition rate estimated by the profilometer was typically 0.25 Å/pulse. X-ray diffraction (XRD) $\theta/2\theta$ scans and θ scans (x-ray ω scans) were used to characterize the epitaxial relationships between the Zn₂Y films, the ZnO buffer layer, and sapphire substrates.

The deposition temperature was optimized in order to obtain epitaxial Zn₂Y thin films. The XRD patterns for films grown at low substrate temperatures (<600 °C) indicated that the films were almost completely amorphous, while the x-ray diffraction data indicated that the films grown at high temperature (900 °C) exhibited epitaxial growth.

The composition of the deposited films was determined using Rutherford backscattering spectroscopy (RBS) analysis as a function of growth temperatures as shown in Table I. Table I shows that films deposited at substrate temperatures

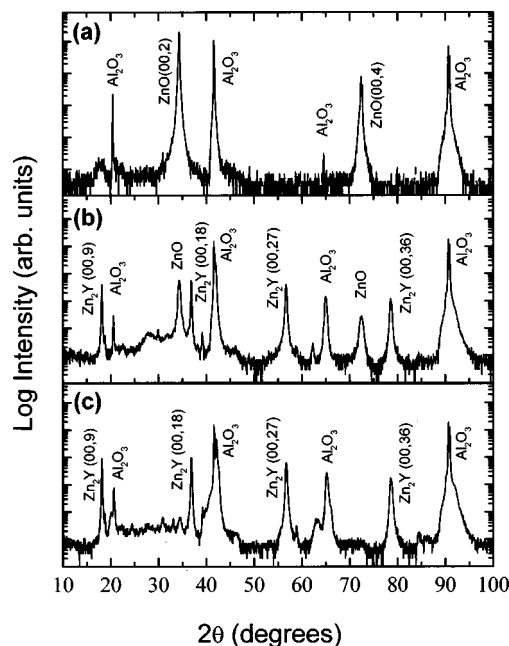


FIG. 1. $\theta/2\theta$ XRD scans for (a) 200-nm-thick ZnO film grown on sapphire at 700 °C in 20 mTorr, (b) as-deposited Zn₂Y film and (c) annealed (at 900 °C in oxygen flow for 2 h) Zn₂Y film (~ 5000 Å) grown on ZnO (~ 400 Å) buffered sapphire at 900 °C in 200 mTorr.

from 700 to 900 °C are deficient in Ba and Zn. The Zn deficiency in the films increased from 65% to 75% with increasing substrate temperature from 700 to 900 °C. Films grown at high temperature were found by XRD to be primarily BaM. Compensation of the target with Ba and Zn (up to 200%) slightly decreased Zn deficiency in the films but did not significantly change the structure of the deposited films whose x-ray diffraction patterns indicate a mixture of Zn₂Y, BaM, and BaFe₂O₄ phases.

In order to reduce the Zn deficiency, we deposited Zn₂Y films on epi-ZnO film on sapphire. The ZnO buffer layer may act as a source of Zn during Zn₂Y film growth. Zn₂Y films were deposited onto epi-ZnO films, which had been grown by PLD onto *c*-Al₂O₃. The epitaxial growth of ZnO on sapphire substrate can be obtained at a substrate temperature from 300–800 °C.^{9,10} However, the optimal growth temperature for the ZnO buffer layer used in this experiment was 700 °C. The full width at half maximum (FWHM) of the x-ray rocking curve for the (002) peak of the ZnO layer decreased with increasing the substrate temperature. The ω (FWHM) for the (002) reflection was 0.25° at 700 °C compared with 0.96° at 300 °C. The x-ray rocking curve did not decrease any more with further increasing the substrate temperature up to 800 °C. The oxygen pressure was optimized to be 20 mTorr for the high quality ZnO films. All ZnO buffer layers used in this experiment were grown at 700 °C in an oxygen background pressure of 20 mTorr. Figure 1(a) shows the x-ray diffraction pattern for a 100 nm ZnO film.

Compensation of the target with excess Zn also improved the Zn₂Y film properties for films deposited on a thin ZnO buffer layer. The composition of the films deposited with the

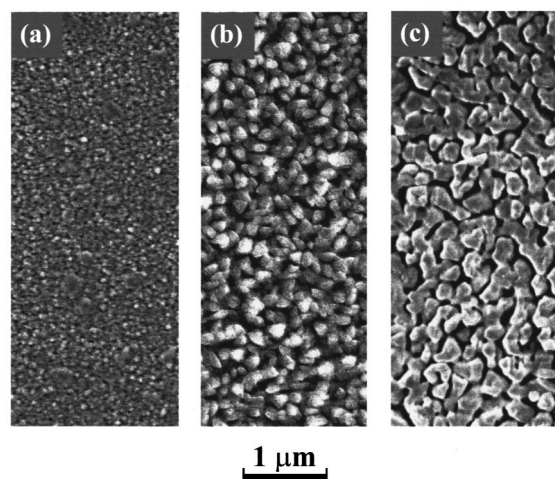


FIG. 2. Scanning electron microscopy photomicrographs of Zn₂Y films deposited in 200 mTorr at deposition temperatures of (a) 600 °C, (b) 700 °C, and (c) 900 °C, respectively.

compensated target (Ba₃Zn₆Fe₁₂O₂₇) was measured by RBS to be Ba_{2.9}Zn_{2.8}Fe₁₂O₂₅. Thus, all of the properties shown in this article are referred to the Zn₂Y films (Ba_{2.9}Zn_{2.8}Fe₁₂O₂₅) deposited with the compensated target on ZnO buffered sapphire substrates.

The crystal quality of the Zn₂Y thin films on ZnO buffered sapphire depends on the substrate deposition temperature. At deposition temperatures less than 600 °C, the x-ray diffraction patterns of the films were observed to be mostly amorphous material. As deposition temperature increased, the Zn₂Y films deposited on ZnO buffered sapphire became highly oriented. The x-ray rocking curve for the (009) peak of the Zn₂Y films deposited at 800 °C on a ZnO buffered sapphire substrate has a FWHM of 0.82°. As the substrate temperature increased to 900 °C, the FWHM of the x-ray rocking curve for the (009) peak narrowed to 0.63°. Moreover, postdeposition annealing of the deposited films decreased the FWHM of the ω scan for the (009) peak to 0.58°.

As shown in Fig. 1(b), the as-deposited film grown on a ZnO buffered sapphire substrate was mainly *c*-axis oriented single phase Zn₂Y. Several impurity peaks were observed at $2\theta=24^\circ, 30.8^\circ, 34.5^\circ, 39^\circ, 59^\circ$ and 63° , respectively. However, their intensities are significantly lower than those of $\langle 001 \rangle$ Zn₂Y film or sapphire substrate diffraction peaks. The impurity peaks have been assigned to ZnO, BaFe₂O₄ and BaM. After post-deposition annealing of the film shown in Fig. 1(b) at 900 °C for 2 hours, the ZnO peaks disappeared as shown in Fig. 1(c). XRD analysis indicated that the *c*-axis lattice parameter of the as-deposited Zn₂Y films grown at 900 °C in 200 mTorr were 43.859 ± 0.057 Å which is larger than the JCPDS¹¹ value of 43.566 Å for the bulk Zn₂Y. This large lattice parameter indicates that the as-deposited Zn₂Y films are under a compressive stress in the film. Differences in lattice parameters between bulk Zn₂Y and Zn₂Y film can be explained by oxygen deficiency^{12,13} and strain effect since there is a significant lattice mismatch and thermal expansion coefficient mismatch between the substrate and film. One

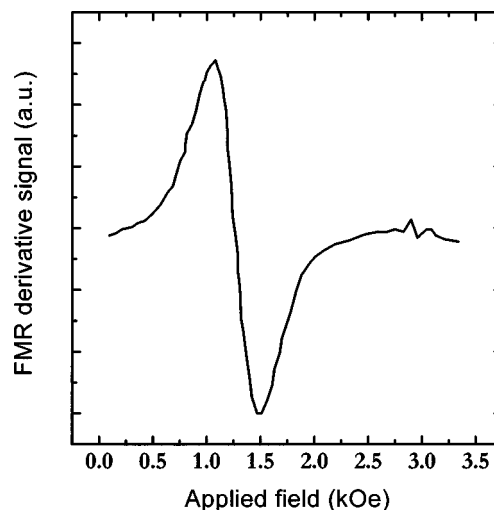


FIG. 3. FMR absorption derivative as a function of static applied field for the film of Fig. 1(c). The static field was applied in plane and the frequency was 9.5 GHz.

other possibility is that the increase in lattice parameter is due to the nonstoichiometric Zn₂Y (Ba_{2.9}Zn_{2.8}Fe₁₂O₂₅) film compared to bulk Zn₂Y (Ba₂Zn₂Fe₁₂O₂₂). However, post-deposition annealing of the deposited films resulted in slight decrease of the lattice parameter to be 43.826 ± 0.054 Å, indicating that the stress in the film was relaxed during annealing due to reduced oxygen deficiency.

The surface morphology of the films was also affected by substrate deposition temperature. As shown in Fig. 2(a), Zn₂Y thin films (~ 5000 Å) deposited at 600 °C were smooth and consisted of nanocrystals (< 50 nm). As the deposition temperature increased up to 900 °C, the grain size of about 250 nm was observed on the surface of the film as shown in Fig. 2(c).

The microwave properties of the Zn₂Y films were characterized by FMR measurements, which were made using a Brüker ECS 109 microwave spectrometer. Fig. 3 shows the FMR absorption derivative versus static applied field for the Zn₂Y film shown in Fig. 1(a). The static applied field was in plane and the frequency was 9.5 GHz. The data were obtained at room temperature. The ferromagnetic resonance (FMR) position at the zero of the peak-to-peak derivative was observed at 1.24 kOe. The FMR derivative linewidth of the as-deposited Zn₂Y film for in-plane applied field was ~ 450 Oe. After postdeposition annealing of the as-deposited Zn₂Y film, the FMR linewidth of the film for in-plane applied field decreased to ~ 310 Oe, which is large compared to that of bulk single-crystal Zn₂Y (18–70 Oe).^{3,7} This large FMR linewidth may be due to the presence of impurities such as BaFe₂O₄ or inhomogeneities in the films. For the perpendicular-to-plane field case, the FMR data showed that the resonance moved up to slightly above 12 kOe, which is the maximum available field of the spectrometer. This indicates that the film has an easy plane of magnetization perpendicular to the *c* axis.

The effective saturation magnetization, $4\pi M_{\text{eff}}$, was estimated using the in-plane FMR field position from the equa-

tion: $f/\gamma = [H_{in}(H_{in} + 4\pi M_{eff})]^{1/2}$, where f is the FMR frequency and γ is the gyromagnetic ratio. With the values of $f=9.5$ GHz, $\gamma=262$ GHz/kOe,³ and $H_{in}=1.24$ kOe, the effective saturation magnetization was estimated to be ~ 9.36 kG. It should be noted that the value of ~ 9.36 kG obtained above may include growth induced anisotropy and contributions from magnetostriction. Assuming that this Zn₂Y film has the same saturation magnetization ($4\pi M_s$) value with the literature value (~ 2850 G)^{3,4} of bulk single-crystal Zn₂Y, the anisotropy (H_a) of this film is about 6.5 kOe, which is smaller than that (9.9 kOe) of the reported^{3,4} bulk single-crystal Zn₂Y.

In conclusion Zn₂Y hexagonal ferrite thin films have been epitaxially grown by PLD. The optimized oxygen pressure and substrate temperature to obtain high quality epitaxial properties of the films were 200 mTorr and 900 °C. The Zn₂Y films (~ 5000 Å) deposited on ZnO (400 Å) buffered *c*-Al₂O₃ substrates with an epitaxial relationship of (001)Zn₂Y// (001)ZnO// (001)Al₂O₃ had a ω -rocking curve FWHM of 0.63° for the (009) peak of the Zn₂Y films. The anisotropy of the Zn₂Y film is estimated to be slightly lower than that of bulk Zn₂Y. The in-plane FMR linewidth of the Zn₂Y film is 310 Oe which is larger than that of bulk single-crystal Zn₂Y.

This work was supported by SPAWAR. The authors thank Ray Auyeung of NRL for his help at the beginning of this project. Also, they would like to thank Professor Carl Patton and Dr. Mike Wittenauer for helpful discussions.

¹J. D. Adams and S. D. Stitzer, IEEE Trans. Microwave Theory Tech. **41**, 2227 (1993).

²J. J. Green and B. J. Healy, J. Appl. Phys. **34**, 1285 (1963).

³W. H. von Aulock, *Handbook of Microwave Ferrite Materials* (Academic, New York, 1965).

⁴W. D. Kingery, H. K. Bowen, and D. R. Uhlmann, *Introduction to Ceramics* (Wiley, New York, 1976).

⁵L. M. Silber, C. E. Patton, and H. F. Naqvi, J. Appl. Phys. **54**, 4071 (1983).

⁶P. Dorsey, K. Sun, C. Vittoria, M. A. Wittenauer, F. J. Friedlander, and A. Schindler, J. Appl. Phys. **67**, 5524 (1990).

⁷M. J. Hurben, D. R. Franklin, and C. E. Patton, J. Appl. Phys. **81**, 7458 (1997).

⁸J. R. Truedson, P. Kabos, K. D. McKinstry, and C. E. Patton, J. Appl. Phys. **76**, 432 (1994).

⁹S. L. King, J. G. E. Gardeniers, and I. W. Boyd, Appl. Surf. Sci. **96-98**, 811 (1996).

¹⁰R. D. Vispute, V. Talyansky, Z. Trajanovic, S. Choopun, M. Downes, R. P. Sharma, T. Venkatesan, M. C. Wood, R. T. Lareau, K. A. Jones, Y. X. Li, and L. Salamanca-Riba, Mater. Res. Soc. Symp. Proc. **474**, 383 (1997).

¹¹See JCPDS Card No. 43-1484.

¹²S. Shin, Mater. Res. Bull. **16**, 299 (1981).

¹³J. Ye and K. Nakamura, Phys. Rev. B **48**, 7554 (1993).

¹⁴L. R. Doolittle, Nucl. Instrum. Methods Phys. Res. B **9**, 344 (1985).